*Desalination and Water Treatment*
www.deswater.com

doi:10.5004/dwt.2018.22119

107 (2018) 28–40
March

# Experimental study on productivity intensification of HDH desalination unit utilizing two-stage dehumidification

Wael M. El-Maghlany[a,*], Ahmed E. Tourab[b], Anwar H. Hegazy[b], Mohamed A. Teamah[a,b], Ahmed A. Hanafy[b]

[a]*Mechanical Engineering Department, Faculty of Engineering, Alexandria University, Egypt, Tel. +201004090302, email: elmaghlany@alexu.edu.eg, elmaghlany@yahoo.com (W.M. El-Maghlany),*
[b]*Mechanical Engineering Department, Arab Academy for Science and Technology and Maritime Transport, Alexandria, Egypt*

Received 6 October 2017; Accepted 26 February 2018

**ABSTRACT**

In this study, an experimental investigation is performed on a two-stage dehumidification water desalination system utilizing a humidification-dehumidification process that has been accomplished using heat pump. The air is heated by means of heat pump condenser to increase its ability to efficiently humidify, while condensation takes place at the heat pump evaporator section. Additionally, in order to enhance the dehumidification efficiency a per-dehumidification process was performed to the humid air, using a cooling water heat exchanger and that was utilized prior to the evaporator. Raw water is sprayed at a constant flow rate of 2.2 L/min using cross, counter, and parallel flow spraying systems. The mass flow ratio between water and air is varied from 0.091 to 0.14 via the change in the air flow rate. The inlet cooling water temperature of the heat exchanger dehumidifier is changed from 15 to 25°C. Results of the experiments showed that the parallel flow spraying system has the highest productivity in both single and two stage dehumidification with a productivity of 2.34 L/h and 4.44 L/h respectively. The results show an extra ordinary influence of the heat exchanger on productivity intensification. The maximum specific productivity including all power consumption elements is 2.02 L/kWh.

*Keywords:* Humidification-dehumidification; Desalination; Heat exchanger; Two-stage dehumidification; Heat pump

## 1. Introduction

Nowadays, fresh water shortage is considered a growing problem that is threatening the world especially that the world population is in continuous increase. As a result, water desalination is considered a sustainable solution to overcome fresh water shortages. Many water desalination technologies are available, the widely used for lagging fresh water production rate are multi-stage flash (MSF), multi-effect evaporation (MEE) and reverses osmosis (RO). These methods require huge amount of energy demand which is mostly covered by fossil fuel. The integration of solar energy with these technologies is a good practice to decrease the reliance on fossil fuel for water desalination. However, solar energy is not highly available with high grade in some regions throughout the year.

A reliable and promising technology that is suitable for low grade energy sources such as solar energy or waste heat is humidification-dehumidification (HDH). It has some advantages such as the capability to operate using low grade heat energy, running under constant pressure, also can be easily installed and maintained, and has a low operating cost, which is suitable for rural remote areas to get fresh water for drinking or irrigation [1]. From the features aforementioned, many researchers are investigating the utilization of solar energy with HDH system. The studies are divided into two main operative manners. The First is air heated system that is used to increase the ability of air to hold more moisture. The second manner is water heated system that is used to humidify the air; other systems may

*Corresponding author.

use both air and water heated. Also, the system can be classified to open or closed air cycle system.

To improve the productivity of a closed air solar water heated system, Kang et al. [2] investigated a two stage multi-effect desalination system. Latent heat of the condensation and heat in the brine water were re utilized to enhance the humidification process. Results showed that the production rate from the fresh water could reach 72.6 kg/h with a gained output ratio of 2.44, due to the utilization of latent heat of condensation and heat in the brine water used. Sharqawy et al. [3] investigated parametrically two HDH desalination systems; air and water heated cycles which can be obtained from low heat source such as solar energy or waste heat sources, to achieve their optimum thermal design and performance with a minimum operating cost. The study concluded that the air heated cycle has larger air pumping power, needs bigger humidifier, and smaller dehumidifier, while the water heated cycle requires larger water pumping power, needs smaller humidifier, and bigger dehumidifier. Li et al. [4] performed an experimental study on the HDH desalination system using evacuated tubes solar air heater. The results show that as the temperature of the sprayed water increases in the pad humidifier, the efficiency of the system increases. Hamed et al. [5] investigated a solar HDH desalination unit theoretically and experimentally during two periods over the course of one day, the first period is from 9 am to 5 pm and the second period is from 1 am to 5 pm. Water was preheated before entering the humidifier. The results showed that the second period had higher productivity at 22 L/d. Mahmoud et al. [6] studied a water desalination system based on HDH theoretically and experimentally using a Fresnel lens in solar water heating. The results show that the rate of evaporation of water could be increased by decreasing water drops diameter. Sharshir et al. [7] experimentally and theoretically studied a hybrid HDH using solar stills. The HDH desalination unit was Closed Air Open Water (CAOW). Results showed that an increase in solar irradiance coincided with an increase in productivity. The average GOR of the HDH unit was 2.14, while for the four solar stills units it approximately equaled 1. Chang et al. [8] performed an experiment on multi-effect solar desalination unit using the HDH process. The cycle performance was enhanced due to the re-utilization of the heat energy in the condensate vapor between the two desalination stages. Gang et al. [9] experimentally studied a multi-effect solar desalination unit using the HDH process. The results show that as the temperature of water increased from 60°C to 90°C and the flow rate of feed water reached 2 ton/h, the production of the freshwater increased from 59.41 to 182.47 kg/h. Giwa et al. [10] investigated a water desalination unit based on HDH process via photo voltaic thermal energy. The results show that the amount of fresh water that could be produced was about 833 with a generated electricity of 278 kWh/. The maximum water production of fresh water was in August which reached 0.528. Orfi et al. [11] experimentally and theoretically investigated an open and closed air loops solar heated desalination unit based on HDH process. The experiments showed that the closed system was better than the open system for production of fresh water. Al-Agouz and Abugderah [12] experimentally studied the parameters affect the humidification process of air by seawater such as water temperature, headwater difference, air velocity. Results showed that the vapor content difference and humidification efficiency increase as the inlet water and air temperatures increase, however they increases as the air velocity decreases. Amer et al. [13] theoretically and experimentally investigated a water desalination unit using HDH process of closed air open water. The circulation of air was both natural and forced. The humidification process has been done using the three different packing materials: gunny pag cloth, wooden slats, and PVC. Li and Zhang [14] experimentally and numerically investigated a solar powered HDH desalination system. 92% of the system energy consumption is covered by solar energy. The unit produces 15.27 kg/d of fresh water with a specific water production of 19.23.

Thermal desalination plants needs to be run with high efficiency and reliable operation. This would be achieved by using a source of heat which consumes a modicum of electric energy and operates without heat loss. The heat pump reduces the consumption of the expensive electric power; in addition to that it can be combined with renewable resources like solar, wind, and geothermal energies. Studies were introduced the use of waste heat with HDH mostly on heat pump system. This integration showed a good potential. Slesarenko [15] proposed the possibility to use heat pumps in the desalination of sea water. The three main types of heat pumps discussed were compression, ejector, and absorption heat pumps. The study concluded that, the absorption heat pumps could be used in high-capacity desalination plants. Ejector heat pumps were of low efficiency while compression heat pumps were efficient for small capacities, as the heat effect generated in the condenser and the cooling effect generated in the evaporator were used. Furthermore other researchers make a use of the air conditioning systems to get fresh water, combining benefits of both air conditioning and desalination systems. Nada et al. [16] introduced an experimental study on HDH desalination system using heat pump. The results showed that the refrigeration load increases as the mass flow rate of air, evaporator saturation air temperature, air specific humidity, and evaporator inlet air temperature increase. The maximum production rate of fresh water was 4.74 kg/h. Gao et al. [17] experimentally studied a desalination unit based on the HDH process using a mechanical vapor compression heat pump, in addition to that a water-cooled heat exchanger placed before the evaporator of the heat pump. The results indicated that as the mass flow rate of the cooling water to the heat exchanger increases, productivity increases. The maximum condensation rate reached was 60 L/d. Hawlader et al. [18] presented an HDH water desalination unit using a solar-assisted heat pump. The experiments showed that the range of the GOR was between 0.77 and 1.15 and the COP for the heat pump ranged from 5.0 to 7.0. The maximum productivity reached was 2.4 kg/h. Yuan et al. [19] experimentally investigated a desalination unit utilizing air conditioning where the air conditioning was derived using a mechanical vapor compression heat pump. The results show that the production of fresh water increases as the sprayed water temperature and flow rate increase. Hegazy et al. [20] performed an experimental study on a desalination unit based on HDH process utilizing heat pump of open air open water (OAOW) air heated system. The humidification process was achieved by spraying water in different flow directions (cross, counter, and parallel). The results show that the cross-flow spraying system achieved the highest rate of evaporation.

Additional HDH investigations [23–31] with their operating conditions are listed in Table 1.

Table 1
Previous research on HDH desalination systems

| Ref. | Maximum productivity | Maximum productivity operating conditions |
|---|---|---|
| Li et al. [4] | 1000 L/d | • Air flow rate = 140 $m^3$/h |
| Mahmoud et al. [6] | 112 L/$m^2$/d | • Closed air loop.<br>• Flow rate per cubic meter of the saline water = 40.8 L/h.<br>• Inlet sea water = 90°C |
| Gang et al. [9] | 22 kg/$m^3$ h | • Heating temperature = 85°C<br>• Feed water rate = 2 t/h. |
| Amer et al. [13] | 5.8 L/h | • Water mass flow rate = 2.8 kg/min.<br>• Water temperature at humidifier inlet = 85°C. |
| Nada et al. [16] | 4.74 kg/h | • Inlet air temperature = 25°C.<br>• Air outlet temperature = 22.71°C. |
| Gao et al. [17] | 5.15 L/d | • Closed air open water.<br>• Air flow rate = 200 kg/h.<br>• Cooling seawater flow rate = 350 kg/h.<br>• Cooling inlet sea water temperature = 18°C.<br>• Solar insolation density = 750 W/$m^2$. |
| Yuan et al. [19] | 2.5 L/h | • Open air open water.<br>• Feed water flow rate = 235 L/h. |
| Kabeel and El-Said [23] | 41.8 kg/d | • Feed water flow rate of HDH = 1 kg/s.<br>• Air flow rate = 0.03 kg/s.<br>• Feed water flow rate of SSF = 0.085 kg/s.<br>• Cooling water flow rate of HDH = 0.1 kg/s.<br>• Cooling water inlet temperature of HDH and SSF = 20°C. |
| Orfi et al. [24] | 27.8 L/$m^2$·d | • Air flow rate = 0.05 kg/s.<br>• Ambient temperature = 33°C.<br>• Sea water temperature = 27°C.<br>• Solar intensity = 930 W/$m^2$.<br>• Sea water flow rate = 0.08 kg/s. |
| El-Shazly et al. [25] | 2 L/h | • Water flow rate = 15 L/min.<br>• Air flow rate = 3.2 $m^3$/h. |
| Hermosillo et al. [26] | 1.45 kg/h | • Saline feed water flow rate = 0.012 kg/s.<br>• Air flow rate = 0.0040 kg/s.<br>• Inlet sea water temperature of the condenser = 27.9°C.<br>• Ambient temperature = 30.5°C. |
| El-Agouz [27] | 8.22 kg/h | • Air flow rate = 14 kg/h.<br>• Inlet sea water temperature = 86°C. |
| Kabeel et al. [28] | 23.6 kg/h | • Inlet water flow rate to the humidifier = 4 kg/min.<br>• Inlet water temperature at humidifier = 90°C. |
| Zhani and Ben Bacha [29] | 21.75 kg/d | • Ambient temperature = 32.75°C.<br>• Air flow rate = 0.01 kg/s.<br>• Water flow rate = 0.04 kg/s.<br>• Inlet water temperature of water solar collector = 37.54°C.<br>• Inlet air temperature of the humidifier = 53.6°C.<br>• Inlet water temperature of the humidifier = 44.69°C.<br>• Solar radiation = 693 W/$m^2$. |
| Farsad and Behzadmehr [30] | 27 kg/h | • Water flow rate = 0.4 to 1.4 kg/s.<br>• Air flow rate = 0.4 to 1.2 kg/s. |
| Ghalavand et al. [31] | 151 kg/h | • Feed sea water flow rate = 1000 kg/h.<br>• Air flow rate = 450 kg/h.<br>• Water to air flow rate ratio = 2.22.<br>• Inlet water temperature = 25°C.<br>• Condenser temperature = 35°C. |
| Present study | 4.44 L/h | • Open air open water.<br>• Parallel flow spraying.<br>• Feed water flow rate = 2.2 kg/min.<br>• Air flow rate = 15.6 kg/min.<br>• Cooling water to the heat exchanger = 4.5 kg/min.<br>• Cooling water temperature to heat exchanger = 15°C. |

## 2. Scope and objective

As mentioned above and up to the author's knowledge, the utilization of an additional dehumidifier heat exchanger in HDH is only limited to the studies that have been performed by Gao et al. [17] and Yuan et al. [19]. However, their results were much closer to specified operating conditions. Also, the HDH units employed an alveolate humidifier with high-pressure drop penalties in the air side and a huge amount of humidification water. The present experimental study with its arrangement is novel. The novelty includes the effect of changing the spraying system configuration on the performance. Also, the water to air ratio is controlled via air, not water. Furthermore, the condenser is air cooled, and the evaporator and heat exchanger are both air heated. In addition to the aforementioned factors, the study resulted in performance enhancement due to the influence of the air mass flow rate on the heat and mass transfer characteristics in the HDH unit components. This due to, the condenser is air cooled; the evaporator and heat exchanger are air heated. Consequently, the humidification, dehumidification efficiencies and the condensation rate are adequate to the HDH components performance. Also, since the air flow rate could be changed, the HDH unit could be used in air conditioning systems. The relative humidity and the temperature of the exiting air from the HDH unit could be adjusted to provide air supply suitable for air conditioning rooms.

## 3. Experimental setup

The system's working principle is based on the statement that air, when heated, can carry a larger amount of water as a humidity content. The heat pump has both necessary heating and cooling effects through both its heat exchanger coils (evaporator and condenser). The desalination process presented in this paper is HDH process of OAOW air heated system. Air is heated via condenser's rejected heat. The hot air is humidified in the humidification section by spraying water. Then, the humidified air enters the dehumidification sections (the heat exchanger and evaporator) to condensate the water vapor. Exit air temperature and humidity could be adjusted to be suitable for air conditioning purposes.

Figs. 1a and 1b show a schematic flow diagram of the built experimental test rig. The air passes through four main sections (A, B, C, and D) with across section

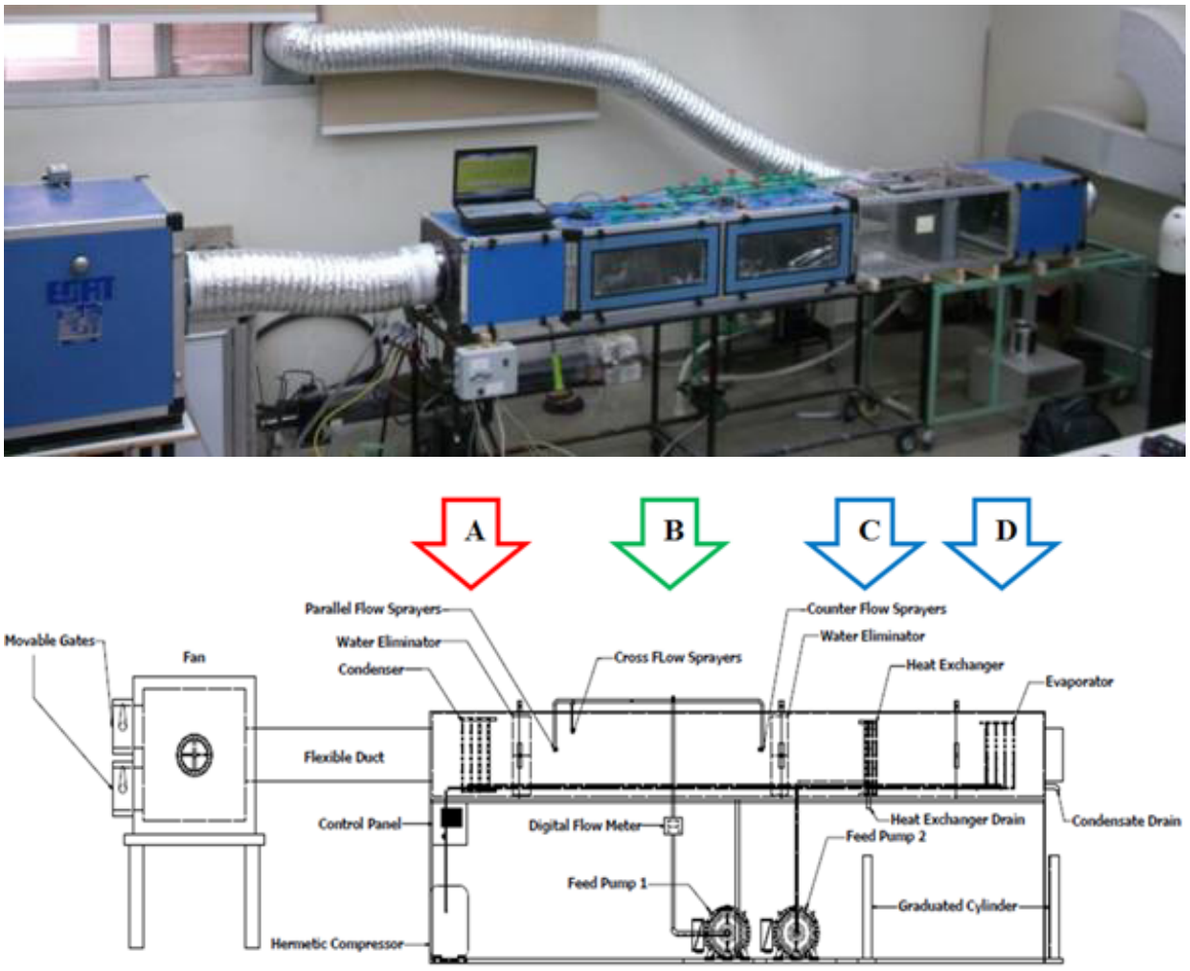


Fig. 1a. Photographic picture for the test rig, b. Schematic diagram for the test rig.

of. First, air is withdrawn to section (A) through a one meter flexible circular duct using a unidirectional centrifugal fan. The fan is fixed in an insulated, galvanized steel box with an air filter in the suction side to avoid any suspended particles. Air flow rates are controlled using two air dampers. In section (A) air is used to condensate the refrigerant (R22) through an aluminum-finned copper coil tube condenser which leads the air's dry bulb temperature to increase. As the dry bulb temperature increases, the air becomes gluttonous to water. Subsequently, air enters through section (B) where the humidification process takes place. The humidification process is accomplished by spraying water via 0.5 HP feed pump (1) with adjusted constant flow rate of 2.2 L/min in three different flowing arrangements; cross, counter, and parallel. After the humidification process, the humidified air goes through a two stage dehumidification process represented in sections (C) and (D) where fresh water is collected. In section (C), a water-cooled aluminum finned tube heat exchanger is fitted. The water is fed at a rate of 4.5 L/min by feed pump (2). The heat exchanger consists of 12 rows and 4 columns and is made of 3/8 inch copper tubes with aluminum fins, as shown in Fig. 2. In section (D), the heat pump evaporator is fitted. The evaporator is constructed from aluminum-finned copper coils. Also, water eliminators are used for the removal of water droplets. Fig. 3a and 3b demonstrate the process flow diagram and the theoretical air processes throughout the experiments on psychometric chart.

## 4. Data collection

Experiments have been carried out on the HDH desalination unit. The productivity of the unit is studied under the steady-state condition. It is found that the unit requires 20 to 30 min for the steady state to be satisfied. At this state, all measured parameters by the instruments are recorded. The dry bulb temperature and relative humidity are measured using a calibrated sensor (DHT 22) before and after each process. The process includes the air heating (condenser), humidification (water sprayers) and two dehumidification processes (heat exchanger and evaporator). The sprayed water flow rate is measured using an electronic turbine digital flow meter. Air mass flow rate is estimated by means of the average air velocity which is measured using a vane anemometer. The measured air velocity distribution across the circular cross-sectional area of the flexible duct along the diameter could be integrated to give the mass flow rate accurately. Each experiment is repeated five times and then the average of the measured data is recorded. The technical specifications of the instrumentation used in the experiments are illustrated in Table 2.

Fixed parameters are taken into consideration during the experiments; the mass flow rate of the sprayed water at

Table 2
Technical specifications of instruments used in experimental set-up

| Measuring instrument | Accuracy | Range |
|---|---|---|
| Testo 416 Telescopic van-anemometer | ± 0.2 m/s | 0.6 to 40 m/s |
| Hanna Instruments HI9564 Thermo-hygrometer | 3 % RH | 20 to 95% RH |
| | ± 0.5°C | 0 to 60°C |
| K24 Electronic turbine Digital flow meter | ± 1.0% | 6 to 120 L/min |
| Digital Temperature & Humidity Sensor Module (DHT22) | 5 % RH | 0–100% |
| | ± 0.5°C | –40 to 80°C |
| Waterproof temperature sensor | ± 0.5°C | –55 to 125°C |
| Obsolete HC-440D Digital Clamp Meter | ± 1.5 % | 0 to 400 Ampere |
| | ± 1.2 % | 0 to 750 Volt |
| E-Type Thermocouple | ± 1.7°C | –270 to 870°C |

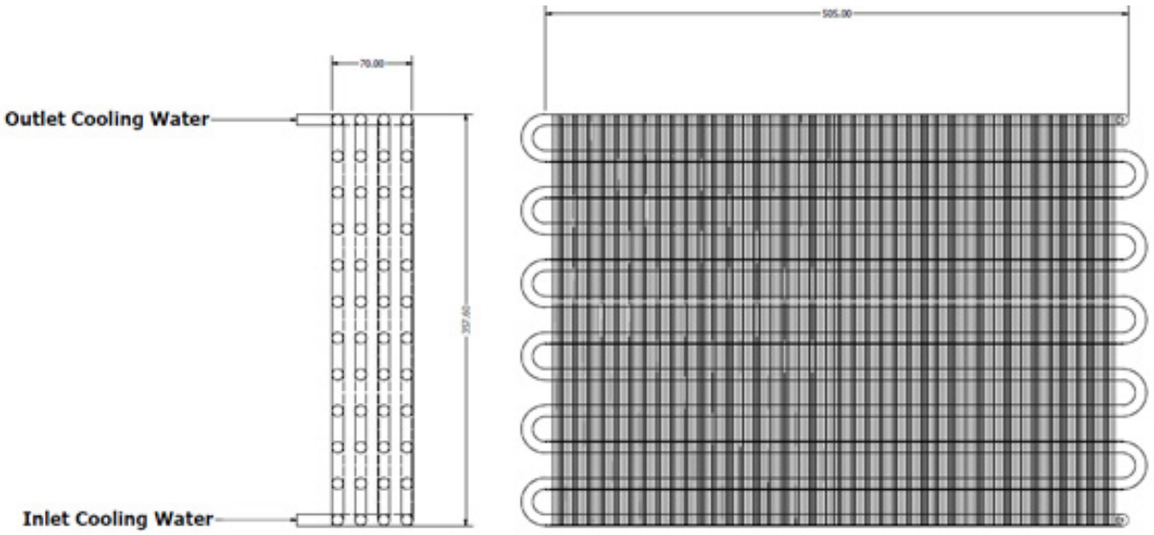


Fig. 2. Schematic diagram for the heat exchanger.

2.2 L/min and the cooling water for the heat exchanger at 4.5 L/min.

## 5. Characteristic equations

The measured data (dry bulb temperature and relative humidity) are used to get the properties of air fr om the psychometric chart at each process as shown in Fig. 3b.

The mass flow rate of air is calculated using the velocity of air that is measured along the cross-sectional area of the circular duct. After that, the velocity profile across the duct is found. From the velocity distribution, air mass flow rate could be found as:

$$\dot{m}_{air} = \int_0^R \rho_{air} V_a dA_r = \int_0^R 2\pi\, r \rho_{air} V_a dr \tag{1}$$

Via the humidity ratio π with the corresponding labeling in Fig. 3a and Fig. 3b, the amount of humidity carried by air due to the humidification process in section (B) is given by:

$$\omega_{Spraying} = \omega_3 - \omega_2 \tag{2}$$

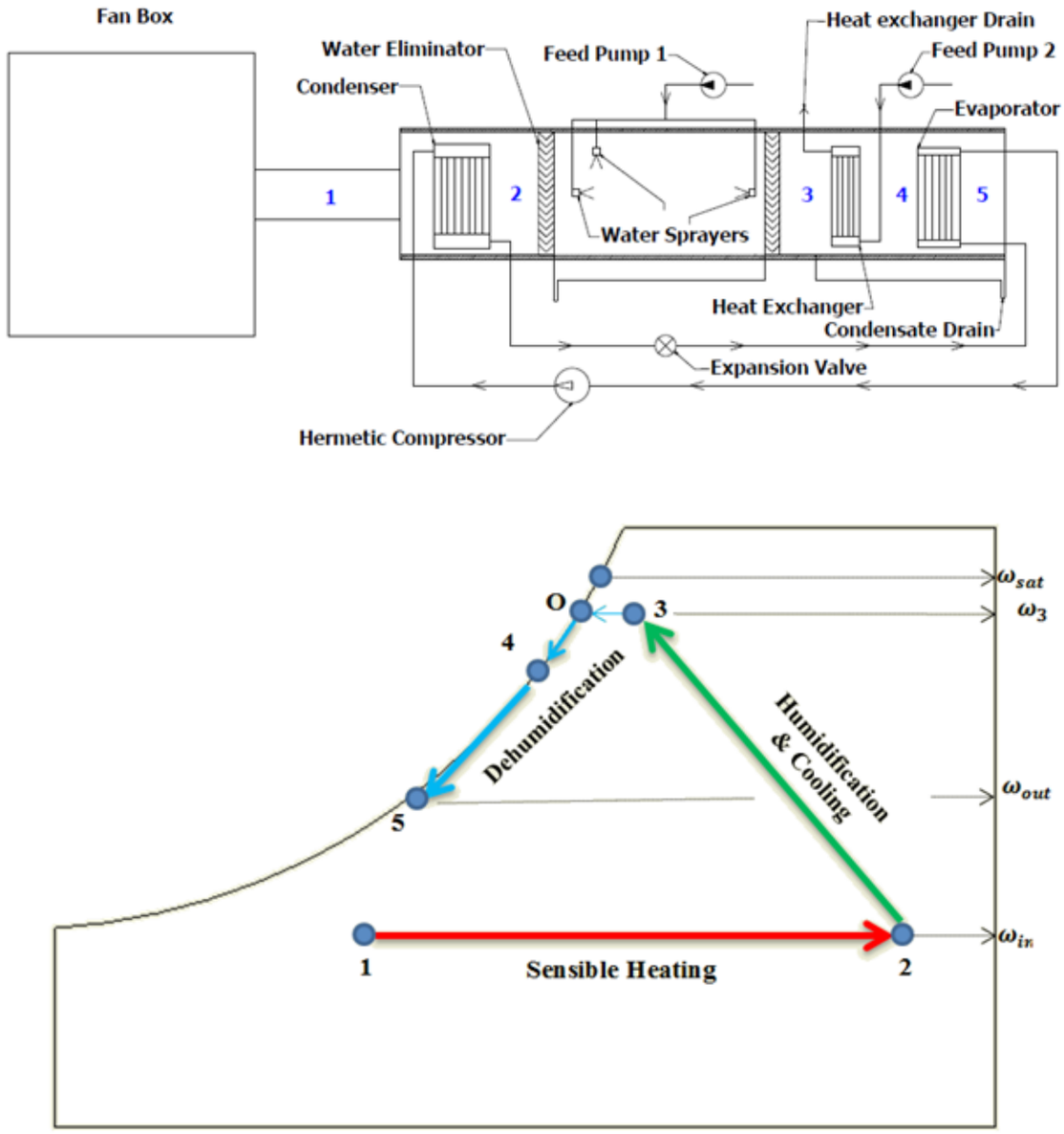


Fig. 3a. Process flow diagram, 3b. Theoretical air processes represented on psychometric chart.

While the amount of humidity withdrawn from air due to the dehumidification process in sections (C) and (D) is:

$$\omega_{Condensate} = \omega_3 - \omega_{out} \tag{3}$$

Consequently, the amount of condensate could be calculated as:

$$\dot{m}_{condansate} = \dot{m}_{air} \times \left(\omega_{Condensate}\right) \tag{4}$$

The humidifier effectiveness is defined as the actual enthalpy variation to the maximum possible enthalpy variation for a heat and mass exchanger [3]:

$$\varepsilon_h = \left[\frac{\left(h_3 - h_2\right)}{\left(h_{a,out,ideal} - h_2\right)}\right] \tag{5}$$

where the ideal outlet air enthalpy is calculated, when the outlet air is dry bulb temperature and specific humidity the same to the inlet ambient air.

Similar to humidifier effectiveness, the dehumidifier is expressed as [3]:

$$\varepsilon_{deh} = \left[\frac{\left(h_3 - h_5\right)}{\left(h_3 - h_{a,out,ideal}\right)}\right] \tag{6}$$

Throughout the experiments, to produce fresh water, the total electrical power consumed by the fan, water pumps, and heat-pump compressor is calculated using as:

$$Electrical\ power = V \times I \times PF \tag{7}$$

One of the important performance parameters in the desalination systems is the gain out ratio (GOR). GOR represents the ration between the required latent heat for the evaporation of desalinated water and the cycle's heat input. This is demonstrated in the following [21]:

$$GOR = \frac{\dot{m}_{condensate} \times h_{fg}}{\dot{Q}_{in}} \tag{8}$$

The heat added to the process by the condenser of the heat pump can be calculated as shown in Fig. 3b:

$$\dot{Q}_{in} = \dot{m}_{air} \times \left(h_2 - h_1\right) \tag{9}$$

## 6. Results and discussion

The experiments have been carried out on the previously described HDH unit. Generalization of the performance of the proposed unit under different working conditions is established. The productivity (benefits) and the energy consumption (penalties) are weighted to get the minimum energy consumption (optimum operating conditions).

By using the root-sum-square method presented by Kline and McClintock [22], the uncertainty values of the studied parameters are estimated. The maximum uncertainties in the condensate rate, electric power, water-to-air mass flow rate ratio and specific productivity are 3.2%, 2.7%, 8.7% and 5.9% respectively.

The unit's performance is tested under three water spraying methods (cross, counter, and parallel) relative to the air flow direction. This process takes place in section (B). The water flow rate remained constant at 2.2 L/min with temperature around 32°C while the air flow rate was controlled. So, the water-to-air mass flow rate ratio is varied from 0.091 to 0.14 via the air mass flow rate regulation. Results are divided into two scenarios. The first scenario involves aone-stage dehumidification process (no heat exchanger) with the evaporator of the heat pump as a condensing surface. The second scenario involves a two-stage-dehumidification process where a water heat exchanger is added before the heat pump evaporator as an additional condensing surface.

The presented results include humidifier effectiveness, dehumidifier effectiveness, condensation rate (productivity), specific productivity and GOR for each case indifferent water spraying modes (cross, counter, and parallel).

### 6.1. One-stage dehumidification process

The results in Figs. 4 to 6 show that for cross, parallel, and counter spraying humidification processes, as the water-to-air mass flow rate increases the condensation rate increases. The condensation rate increases as the air flow rate decreases up to a water-to-air ratio of 0.135. The condensation rate after this ratio tends to decrease for parallel and counter flows, while for the cross flow almost it tends to be constant. Parallel water spraying yields the highest condensation rate compared to cross and counter water spraying. This behavior could be explained with respect to the humidifier effectiveness. With good atomization in the sprayers, the contact length is larger in the parallel flow and consequently,the humidifier effectiveness is enhanced, Fig. 5. The maximum water production rate is found to be 2.34 L/h at parallel spraying humidification with a water-to-air mass flow rate of 0.138.

Comparing Fig. 4 with Fig. 5, it can be concluded that the humidifier effectiveness has a major influence on the system's productivity. It is clear that both curves in all water spraying regimes have the same trend. As the water-to-air ratio increases, the humidifier effectiveness increases till an optimum value at a mass flow rate ratio of 0.138, which corresponds to the maximum condensation rate for one stage dehumidification process.

One major concept should be taken into consideration in the analysis of HDH. As the effectiveness of the humidification process increases, the dehumidifier effectiveness accordingly increases. The increase in humidifier effectiveness leads to relatively high humidity of the exit air (point 3). So, the sensible cooling load on the evaporator decreases (process 3-O), and the condensation efficiency is enhanced, which leads to high productivity. This relation can be observed in Fig. 6. It shows that as the water-to-air ratio increases, the dehumidifier effectiveness increases due to the increase in the air's relative humidity at the entrance of the dehumidification process, Fig. 7. However, the dehumidifier effectiveness is relatively low with a maximum value of approximately 48.9%. This weak effectiveness is due to the high cooling load on the evaporator as it is the only cold surface conducive to condensation. The large gap between both humidifier and dehumidifier effective-

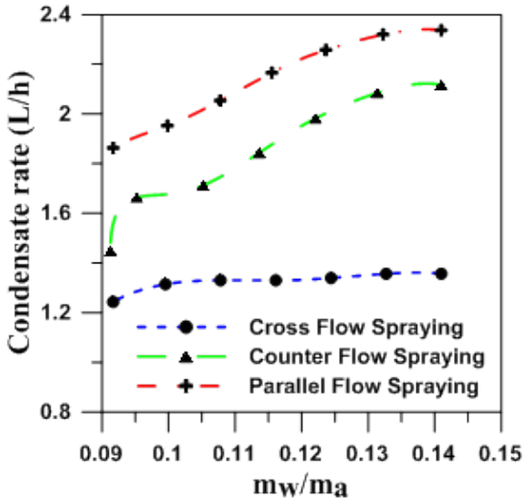


Fig. 4. Condensate rate in single-stage dehumidification.

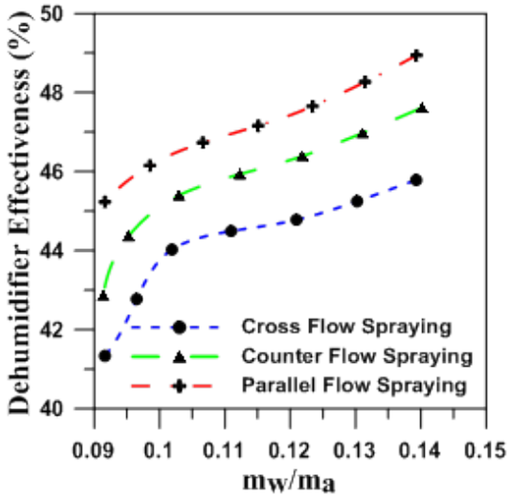


Fig. 6. Dehumidifier effectiveness in single-stage dehumidification.

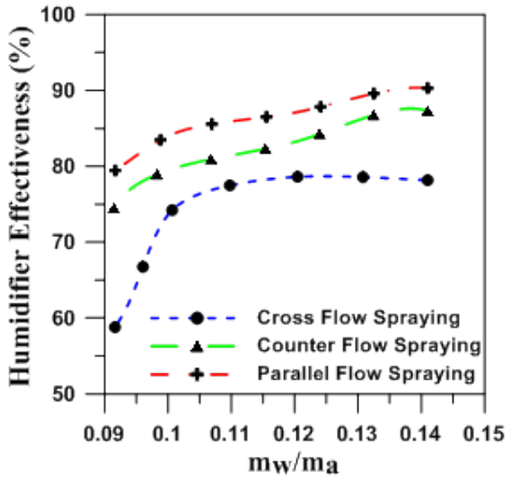


Fig. 5. Humidifier effectiveness in single-stage dehumidification.

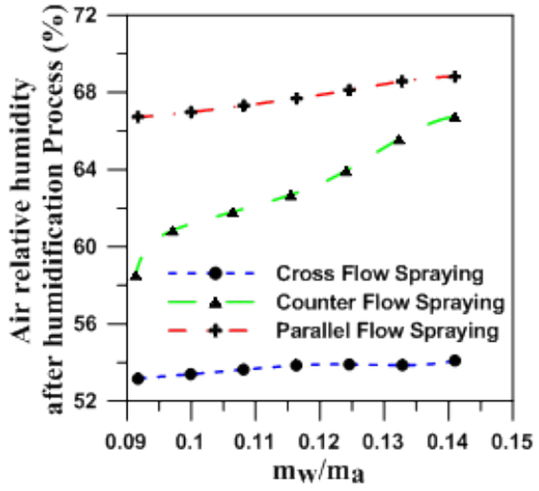


Fig. 7. Air relative humidity at the humidifier outlet.

ness could be collapsed via the cooling load reduction in the evaporator by an assisted cold surface for pre-condensation. Therefore, an additional heat exchanger is used to improve the dehumidification process and consequently, productivity intensification (aim of the present study).

### 6.2. Two-stage dehumidification process

A water heat exchanger is added as an additional condensing surface before the heat pump's refrigerant heat exchanger (evaporator). As a result, the dehumidification is accomplished through two stages. The increase in the cooling capacity (evaporator and heat exchanger) leads to a desired enhancement in the dehumidifier effectiveness, Fig. 8. As shown in Fig. 8, the heat exchanger augments the performance of the HDH unit in the different case studies (cross, counter and parallel water spraying) compared to the single stage dehumidification. Also, the inlet cooling water temperature to the heat exchanger has an extra ordinary effect on the dehumidifier effectiveness. Experiments with low water temperature have higher dehumidifier effectiveness as shown in Fig. 8 at 15°C, 17.5°C, 20°C, 22.5°C and 25°C. It should be denoted that the cooling water inlet temperature to the heat exchanger is corresponding to the ambient water temperature available, that varies through the year. The inlet water temperature is close to the wet bulb temperature of the atmospheric air. So, year round, the heat exchanger could be utilized without any additional cooling cost with performance depending on the outside air condition. The effectiveness of the dehumidification process increases as the water-to-air mass flow rate ratio increases till a peak of 0.122 and after that tends to decrease at low inlet water temperature to the heat exchanger. This behavior could be explained as, in the present study; the water-to-air mass flow rate ratio has been changed via the air flow rate, while the sprayed water is held constant. As the water-to-

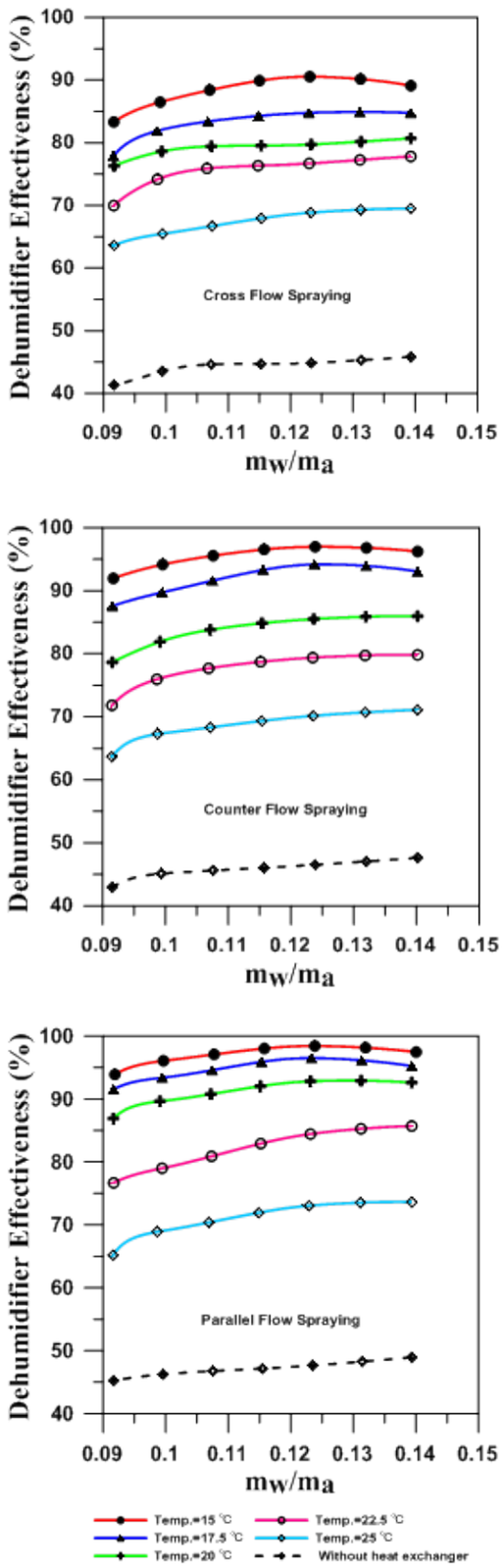


Fig. 8. Dehumidifier effectiveness in one and two stage dehumidification process for the three flow spraying orientations.

air mass flow rate ratio excessively increases, the air flow rate sharply decreases. Consequently, the Reynolds number decreases and weak heat transfer coefficient is found. The heat transfer rate from humidified air to the dehumidifier is reduced and the condensate rate is reduced also. So, it is recommended to adjust the air flow rate to get the peak condensation rate.

Fig. 9 represents the condensation rate of the unit against the water-to-air mass flow rate ratios for one-stage and two-stage dehumidification processes with parallel mode appearing to be the most suitable. The two-stage dehumidification process proved to boost the unit's productivity. The maximum productivity reached was 4.44 L/h. This was achieved under the following conditions: parallel humidification process, the cooling water entering the heat exchanger was at a temperature 15°C, and the water-to-air ratio was 0.122. The enhancement in the dehumidifier effectiveness is addressed to the means of higher condensation rate which means better productivity from the unit. The condensate rate, Fig. 8, is strongly related to the dehumidifier effectiveness, Fig. 8.

An important measure of the system is the power consumption needed for fresh water production. The total consumed power is the summation of the electric power of the fan, heat pump, and the water pumps. Fig. 10 presents the condensation rate per kWh (specific productivity) against the water-to-air mass flow rate ratio in one-stage and two-stage dehumidification process for cross, counter and parallel water spraying humidification directions. The optimum water condensation rate from the power consumption viewpoint is 2.02 L/kWh in parallel flow spraying in two-stage dehumidification process at an inlet cooling water temperature of 15°C to the heat exchanger.

The performance of the desalination unit is evaluated by GOR. Fig. 11 shows the GOR versus water-to-air mass flow rate ratios for one and two stage dehumidification processes in cross, counter,and parallel flow spraying. The heat exchanger improves the performance of the unit as is clear in Fig. 11.As the inlet cooling water temperature decreases, the GOR increases, thereby productivity increases with respect to the added heat energy. The maximum GOR at the optimum operating condition is 1.34. The peak GOR increases sharply from 0.33 (no heat exchanger) to 1.34 (with heat exchanger) due to the utilization of the heat exchanger.

Table 1 depicts a summary of some works, including the present study, on water desalination using HDH process. The data represents the maximum productivity with its operating conditions.

## 7. Comparison between the proposed and previous HDH systems

Fig. 12 shows a comparison between the present study in the case of parallel flow with two stage dehumidification and Yuan et al. [19]. There is significant similarity between both systems' performance behaviors. As the water-to-air ratio increases, the rate of condensate also increases. However, the new system is more efficient. The condensation rate is higher than Yuan et al. [19] not only in its value, but also at a lower water-to-air ratio. This is due to the fact that in the present study, the water-to-air ratio is controlled by means of air flow rate which has a major influence on the

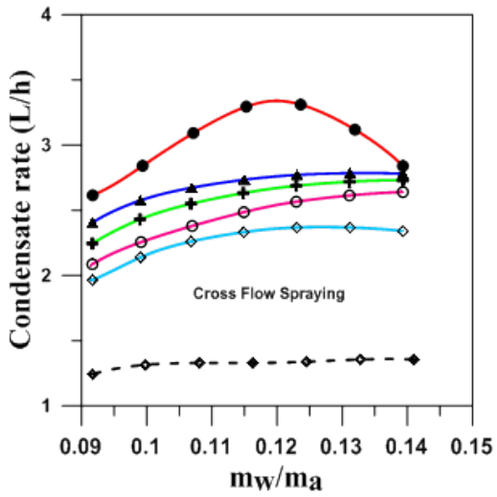


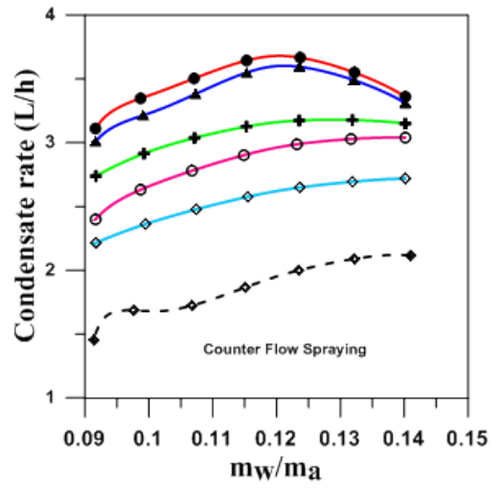


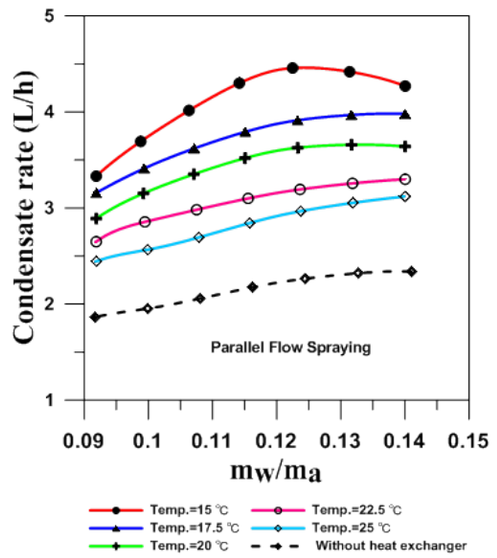


Fig. 9. Condensate rate in one and two stage dehumidification process for the three flow spraying directions.

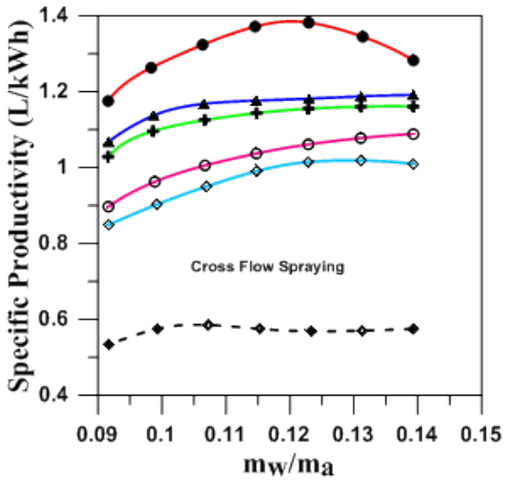


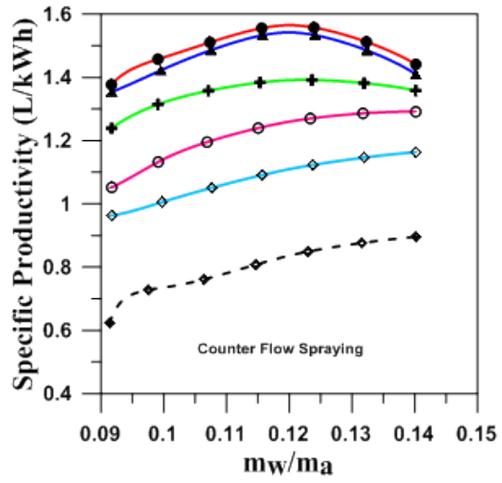


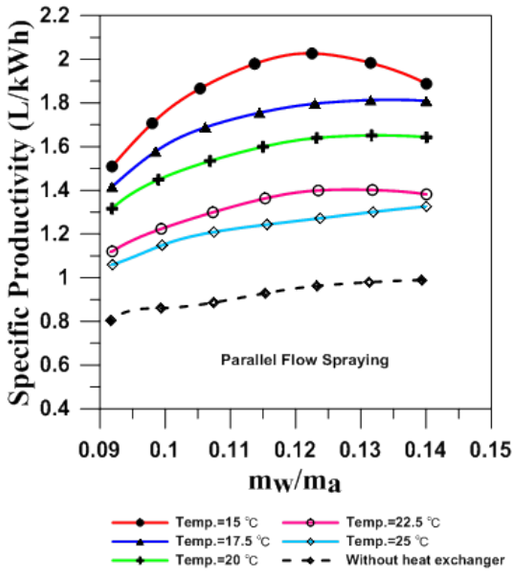


Fig. 10. Specific productivity of the unit in one and two stage dehumidification process for the three flow spraying directions.

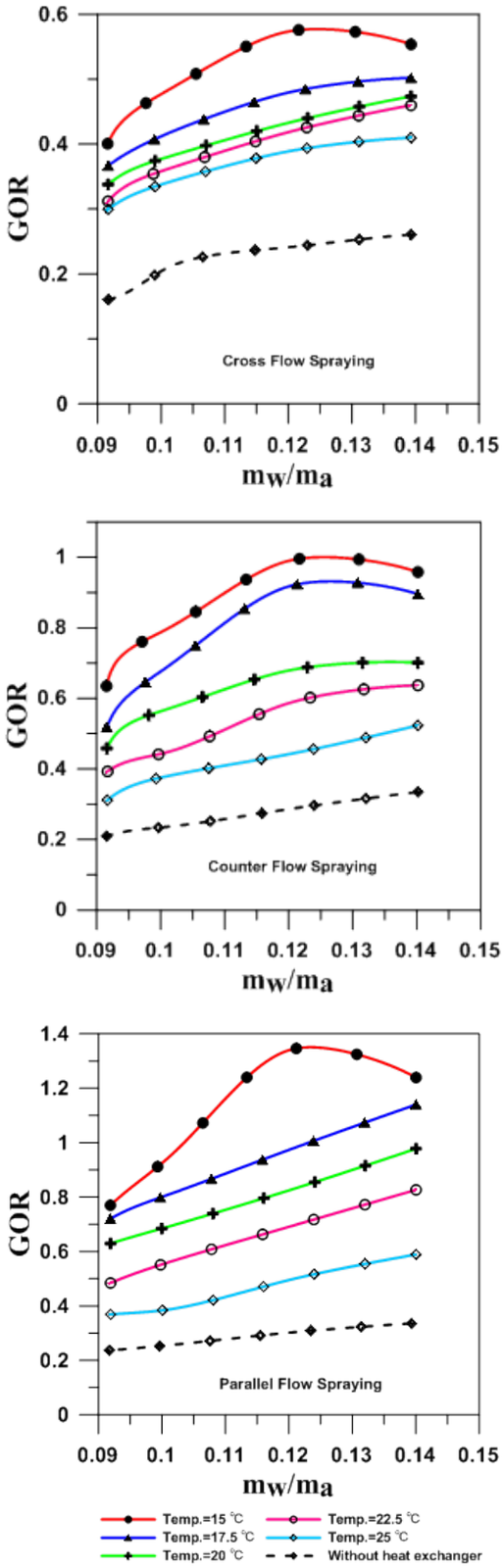


Fig. 11. GOR of the unit in one and two stage dehumidification process for the three flow spraying directions.

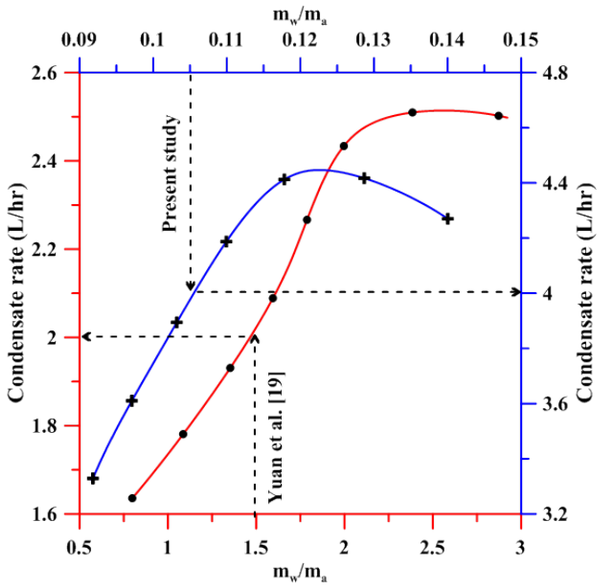


Fig. 12. Comparison between present study and Yuan et al. [19].

HDH unit components. The air couples the condenser, the heat exchanger and the evaporator with the humidifier in their performances. In other words the heat transfer is related directly to the mass transfer adequately. Also, in the present study, the amount of sprayed water that is theoretically absorbed by the air is controlled, while the humidification by an alveolate humidifier [19] needs a large amount of water due to the absence of the atomization that is generated through sprayers (the present study).

## 8. Conclusion

In this experimental work, a water desalination unit based on HDH process using heat pump is investigated. The results include the effect of water flow spraying directions (cross, counter, and parallel flows) at different air mass flow rates. The experiments were conducted under two scenarios. The first scenario involved single-stage dehumidification, while the second involved two-stage dehumidification using a heat exchanger placed before the evaporator of the heat pump and the utilization of different inlet cooling water temperatures. Results of the present study revealed that:

- The parallel flow spraying system has the highest productivity in both single and two stage dehumidification with a productivity of 2.34 L/h and 4.44 L/h respectively.
- The dehumidification efficiency increases as the water-to-air mass ratio increases.
- The temperature of the inlet cooling water to the heat exchanger has a great effect on the dehumidification efficiency; the lower the temperature, the greater the dehumidification efficiency.
- The maximum specific productivity is 2.02 L/kWh, with peak GOR of 1.34.

- The preferable operating condition is at an inlet cooling water temperature of 15 to the heat exchanger and a water-to-air mass ratio of 0.122 using the parallel flow spraying orientation.

## Symbols

| | | |
|---|---|---|
| $A_{cross}$ | — | Cross-sectional area ($m^2$) |
| $h$ | — | Specific enthalpy (kJ/kg) |
| $h_{fg}$ | — | Latent heat (kJ/kg) |
| $I$ | — | Electric current (A) |
| $\dot{m}_{air}$ | — | Air mass flow rate (kg/s) |
| $\dot{m}_{condensate}$ | — | Condensate mass flow rate (kg/s) |
| $\dot{Q}_{in}$ | — | Heat added to the cycle (kW) |
| $r$ | — | The air duct local radius (m) |
| $R$ | — | The air duct inner radius (m) |
| $V$ | — | Voltage (V) |
| $V_a$ | — | Local measured air velocity (m/s) |

## Abbreviations

| | | |
|---|---|---|
| a | — | Air |
| CAOW | — | Closed air open water |
| COP | — | Coefficient of performance |
| GOR | — | Gain output ratio |
| HDH | — | Humidification-dehumidification |
| $m_w/m_a$ | — | Water sprayed to air flow mass ratio |
| MEE | — | Multi-Effect Evaporation |
| MSF | — | Multi-Stage Flash |
| OAOW | — | Open air open water |
| PF | — | Power factor |
| RH | — | Relative humidity (%) |
| RO | — | Reverses Osmosis |
| SSF | — | Single Stage Flashing |

## Greek

| | | |
|---|---|---|
| $\varepsilon_h$ | — | Humidifier effectiveness |
| $\varepsilon_{deh}$ | — | Dehumidifier effectiveness |
| $\omega$ | — | Humidity ratio ($kg_w$/ $kg_{air}$) |
| $\rho_{air}$ | — | Air density ($kg/m^3$) |

## References


[1] W. Gang, H. Zheng, H. Kang, Y. Yang, P. Cheng, Z. Chang, Experimental investigation of a multi-effect isothermal heat with tandem solar desalination system based on humidification–dehumidification processes, Desalination, 378 (2016) 100–107.

[2] H. Kang, Y. Yang, Z. Chang, H. Zheng, Z. Duan, Performance of a two-stage multi-effect desalination system based on humidification–dehumidification process, Desalination, 344 (2014) 339–349.

[3] M.H. Sharqawy, M.A. Antar, S.M. Zubair, A.M. Elbashir, Optimum thermal design of humidification dehumidification desalination systems, Desalination, 349 (2014) 10–21.

[4] X. Li, G. Yuan, Z. Wang, H. Li, Z. Xu, Experimental study on a humidification and dehumidification desalination system of solar air heater with evacuated tubes, Desalination, 351 (2014) 1–8.

[5] M.H. Hamed, A.E. Kabeel, Z.M. Omara, S.W. Sharshir, Mathematical and experimental investigation of a solar humidification–dehumidification desalination unit, Desalination, 358 (2015) 9–17.

[6] M.S. Mahmoud, T.E. Farrag, W.A. Mohamed, Experimental and theoretical model for water desalination by humidification - dehumidification (HDH), Procedia Environ. Sci., 17 (2013) 503–512.

[7] S.W. Sharshir, G. Peng, N. Yang, M.A. Eltawil, M.K.A. Ali, A.E. Kabeel, A hybrid desalination system using humidification-dehumidification and solar stills integrated with evacuated solar water heater, Energy Convers. Manage., 124 (2016) 287–296.

[8] Z. Chang, H. Zheng, Y. Yang, Y. Su, Z. Duan, Experimental investigation of a novel multi-effect solar desalination system based on humidification–dehumidification process, Renew. Energy, 69 (2014) 253–259.

[9] W. Gang, H. Zheng, H. Kang, Y. Yang, P. Cheng, Z. Chang, Experimental investigation of a multi-effect isothermal heat with tandem solar desalination system based on humidification–dehumidification processes, Desalination, 378 (2016) 100–107.

[10] A. Giwa, H. Fath, S.W. Hasan, Humidification–dehumidification desalination process driven by photo voltaic thermal energy recovery (PV-HDH) for small-scale sustainable water and power production, Desalination, 377 (2016) 163–171.

[11] J. Orfi, M. Laplante, H. Marmouch, N. Galanis, B. Benhamou, S.B. Nasrallah, C.T. Nguyen, Experimental and theoretical study of a humidification-dehumidification water desalination system using solar energy, Desalination, 168 (2004) 151–159.

[12] S.A. El-Agouz, M. Abugderah, Experimental analysis of humidification process by air passing through seawater, Energy Convers. Manage., 49 (2008) 3698–3703.

[13] E.H. Amer, H. Kotb, G.H. Mostafa, A.R. El-Ghalban, Theoretical and experimental investigation of humidification–dehumidification desalination unit, Desalination, 249 (2009) 949–959.

[14] G.-P. Li, L.-Z. Zhang, Investigation of a solar energy driven and hollow fiber membrane-based humidification–dehumidification desalination system, Appl. Energy, 177 (2016) 393–408.

[15] V.V. Slesarenko, Heat pumps as a source of heat energy for desalination of seawater, Desalination, 139 (2001) 405–410.

[16] S.A. Nada, H.F. Elattar, A. Fouda, Experimental study for hybrid humidification–dehumidification water desalination and air conditioning system, Desalination, 363 (2015) 112–125.

[17] P. Gao, L. Zhang, H. Zhang, Performance analysis of a new type desalination unit of heat pump with humidification and dehumidification, Desalination, 220 (2008) 531–537.

[18] M.N.A. Hawlader, P.K. Dey, S. Diab, C.Y. Chung, Solar assisted heat pump desalination system, Desalination, 168 (2004) 49–54.

[19] G. Yuan, L. Zhang, H. Zhang, Experimental research of an integrative unit for air-conditioning and desalination, Desalination, 182 (2005) 511–516.

[20] A.H. Hegazy, M.A. Teamah, A.A. Hanafy, Wael M. EL-Maghlany, experimental study of a water desalination system based on humidification-dehumidification process using a heat pump, International Mechanical Engineering Congress and Exposition, Houston, Texas, (2015) 13–19.

[21] G.P. Narayan, M.H. Sharqawy, J.H.V. Lienhard, S.M. Zubair, Thermodynamic analysis of humidification dehumidification desalination cycles, Desal. Water Treat., 16 (2010) 339–353.

[22] S. Kline, F. Mcclintock, Describing uncertainties in single-sample experiments, Mech. Eng., 75 (1953) 3–8.

[23] A.E. Kabeel, E.M.S. El-Said, A hybrid solar desalination system of air humidification, dehumidification and water flashing evaporation: Part II. Experimental investigation, Desalination, 341 (2014) 50–60.

[24] J. Orfi, N. Galanis, M. Laplante, Air humidification–dehumidification for a water desalination system using solar energy, Desalination, 203 (2007) 471–481.

[25] A.H. El-Shazly, A.A. Al-Zahrani, Y.A. Alhamed, S.A. Nosier, Productivity intensification of humidification–dehumidification desalination unit by using pulsed water flow regime, Desalination, 293 (2012) 53–60.

[26] J. Hermosillo, C.A. Arancibia-Bulnes, C.A. Estrada, Water desalination by air humidification: Mathematical model and experimental study, Solar Energy, 86 (2012) 1070–1076.

[27] S.A. El-Agouz, A new process of desalination by air passing through seawater based on humidification–dehumidification process, Energy, 35 (2010) 5108–5114.
[28] A.E. Kabeel, M.H. Hamed, Z.M. Omara, S.W. Sharshir, Experimental study of a humidification-dehumidification solar technique by natural and forced air circulation, Energy, 68 (2014) 218–228.
[29] K. Zhani, H.B. Bacha, Experimental investigation of a new solar desalination prototype using the humidification dehumidification principle, Renew. Energy, 35 (2010) 2610–2617.
[30] S. Farsad, A. Behzadmehr, Analysis of a solar desalination unit with humidification–dehumidification cycle using DoE method, Desalination, 278 (2011) 70–76.
[31] Y. Ghalavand, M.S. Hatamipour, A. Rahimi, Humidifi cation compression desalination, Desalination, 341 (2014) 120–125.